Electronic Supplementary Information (ESI)

P-doped binary Ni/Fe-N-C for enhanced oxygen electrocatalysis performance

Hongrui Jia[a], Xiangshe Meng[a], Yan Lin[a], Danni Wang[a], Guoqiang Li*[,a], and Guoxin Zhang*[,a]

a. College of Energy Storage Technology, Shandong University of Science and Technology, Qingdao, Shandong 266590, China. E-mail: ligq@sdust.edu.cn, zhanggx@sdust.edu.cn

1. Experimental Section

1.1. Chemicals and reagents

Zinc chloride ($ZnCl_2$, A.R. grade), ferrous chloride ($FeCl_2$, A.R. grade), nickel chloride ($NiCl_2$, A.R. grade), phenylphosphonamide ($C_6H_9N_2O_2P$, PPPA) and RuO_2 were bought from Shanghai Macklin Biochemical Co., Ltd. Formamide (CH_3NO, FA, purity > 99%) was brought from Tianjin Damao Chemical. KOH, absolute ethanol and methanol were purchased from Sinopharm Chemical Reagent Co., Ltd. Nafion solution (5.0 wt%, Dupont) and commercial Pt/C (20.0 wt%) were bought from Shanghai Hesen Electric Co., Ltd. Conductive carbon black was bought from XFNANO, Inc. All reagents were used without further purification.

1.2. Characterizations

X-ray diffraction (XRD) was performed on a Brüker D8 Advance diffractometer at 40 kV and 40 mA using Cu Kαradiation (λ= 0.15406 nm). Scanning electron microscopy (SEM) was performed on an Apreo S HiVac scanning electron microscope at an acceleration voltage of 15 kV. Transmission electron microscopy (TEM), high-resolution TEM (HRTEM), and High-angle annular dark-field scanning transmission electron microscopy (HAADF-STEM) were performed with a FEI Talos 200S high-resolution transmission electron microscope at an acceleration voltage of 200 kV. Raman spectra were obtained by a DXR2 Raman Microscope (Thermo Fisher) with 532 nm line of Ar laser as the excitation source. X-ray photoelectron spectrum (XPS) analysis was performed on a PHI 5000 Versaprobe system using monochromatic Al Kαradiation (1486.6 eV). The specific surface area and pore

distribution were determined through N_2 gas adsorption/desorption measurements (ASAP 2020, Micromeritics Instrument Corporation, USA).

1.3. Electrochemical measurements

Electrochemical measurements of ORR and OER performance were conducted on a home-made three-electrode electrochemical setup using saturated calomel electrode (Hg/Hg_2Cl_2, with saturated KCl solution) as the reference electrode, carbon rod as the counter electrode, and catalyst-loaded glassy carbon electrode (GCE) as the working electrode. The three-electrode system connected with the CHI 760e electrochemical station (Shanghai Chenhua Co., Ltd., China) and worked at room temperature. For the preparation of catalyst ink, 5.0 mg of catalyst, 1.0 mg of conductive carbon black, and 10.0 μL of Nafion solution (5.0 wt%) were mixed in 500 μL absolute ethanol, then thoroughly sonicated to obtain homogeneous suspension. The as-prepared ink was casted on a glass carbon rotation disk electrode (RDE) with the catalyst loading of 0.10 mg cm^{-2}.

Electrochemical measurements for ORR were performed in 0.1 mol L^{-1} KOH electrolyte. ORR cyclic voltammetry (CV) tests were performed using the scanning rate of 50.0 mV s^{-1} and linear sweep voltammetry (LSV) tests at 5.0 mV s^{-1}. Before all the ORR tests, O_2 gas were purged in the electrolyte for 30 min to reach O_2 saturation and maintained purging during all the ORR tests. All the potentials were normalized to the potential of the reversible hydrogen electrode (RHE). ORR polarization curves were collected with different rotating speeds. Koutecky-Levich (K-L) plots were then obtained using potentials from the ORR LSV curves at different

potentials. The ORR electron transfer number can be determined using K-L equations.

$$\frac{1}{J}=\frac{1}{J_L}+\frac{1}{J_K}=\frac{1}{B\omega^{1/2}}+\frac{1}{J_K} \quad (1)$$

$$B=0.62nFC_0D_0^{2/3}v^{-1/6} \quad (2)$$

Tafel slopes were calculated using ORR LSV curves following the Tafel equation below.

$$\eta=a+b\times log|j| \quad (3)$$

The EIS measurements were conducted on an Autolab potentiostat in the frequency range of 0.1 Hz to 100 kHz, a 10 mV amplitude of sinusoidal potential perturbation was employed in the measurements.

OER measurements were performed in an oxygen-saturated 1.0 mol L^{-1} KOH electrolyte with the scanning rate of 50.0 mV s^{-1} for CV and 5.0 mV s^{-1} for LSV. Commercial platinum carbon (Pt/C, 20 wt%) and RuO_2 were used for comparing the ORR and OER performance of the as-prepared samples.

2. Figures and Tables

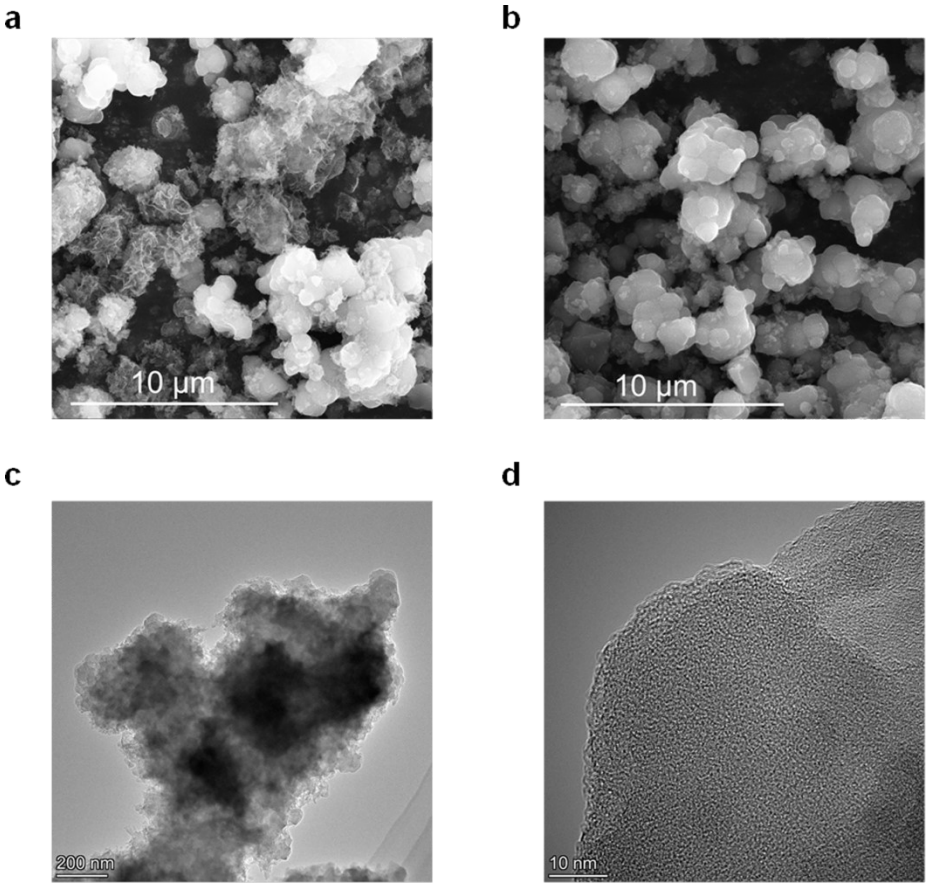

Fig. S1 SEM images of different precursors: (a) f-NiFe-NC, (b) f-Zn-NC, (c, d) TEM images of f-NiFe-NC.

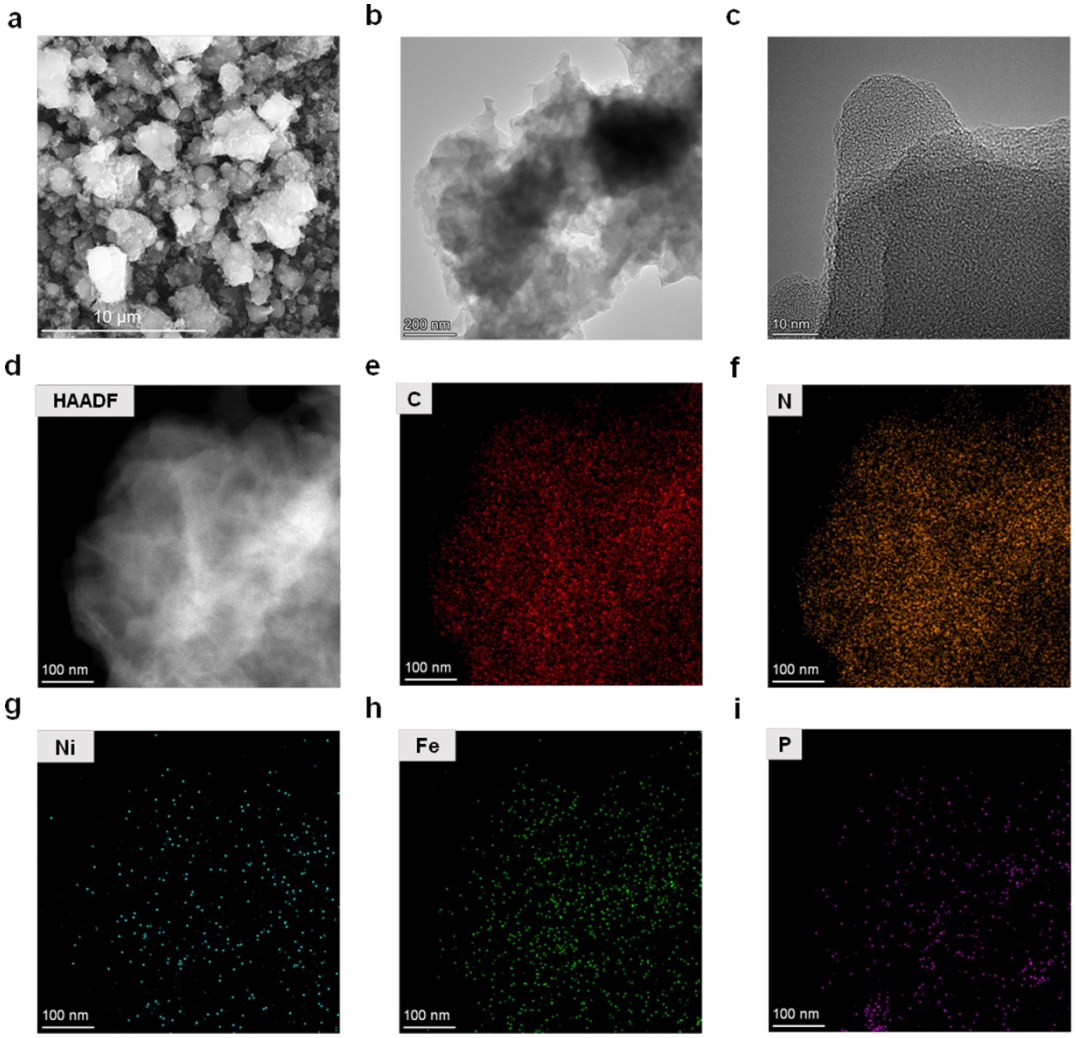

Fig. S2 (a) SEM image of f-P-NiFe-NC. (b, c) TEM images of f-P-NiFe-NC. (d-i) HAADF-STEM and corresponding EDS mapping images of f-P-NiFe-NC.

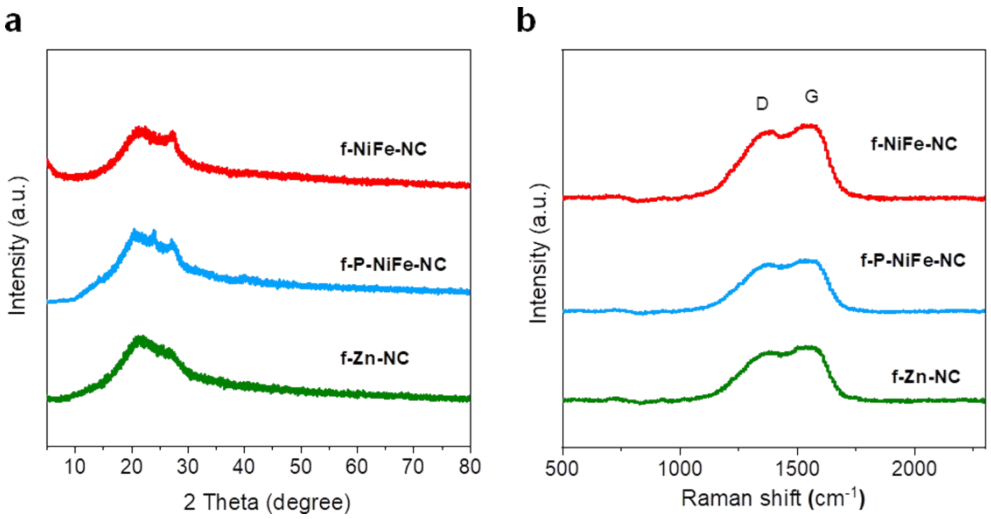

Fig. S3 (a) XRD curves and (b) Raman spectra of f-NiFe-NC, f-P-NiFe-NC and f-Zn-NC.

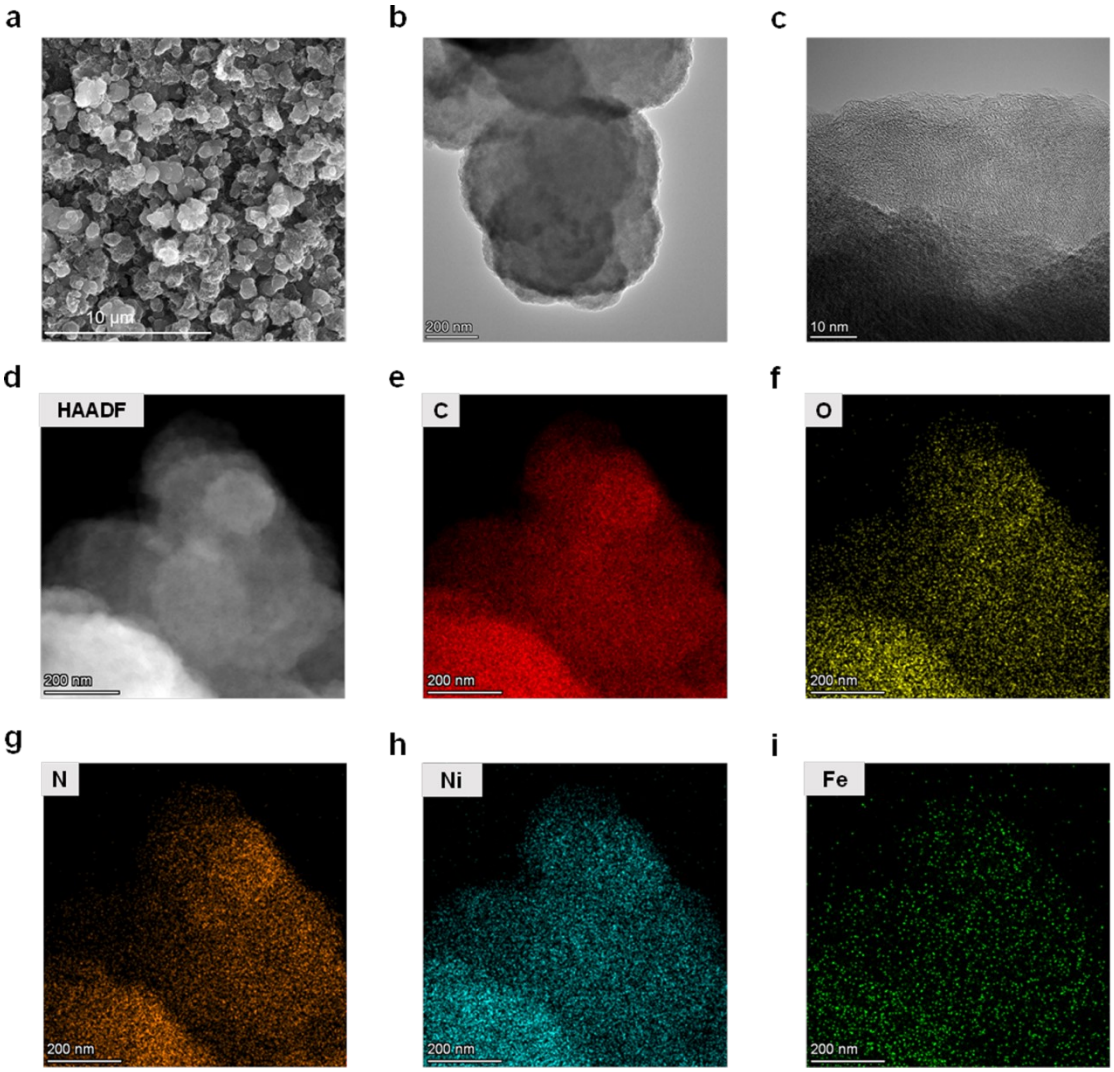

Fig. S4 (a) SEM image of NiFe-NC. (b, c) TEM images of NiFe-NC. (d-i) HAADF-STEM and corresponding EDS mapping images of NiFe-NC.

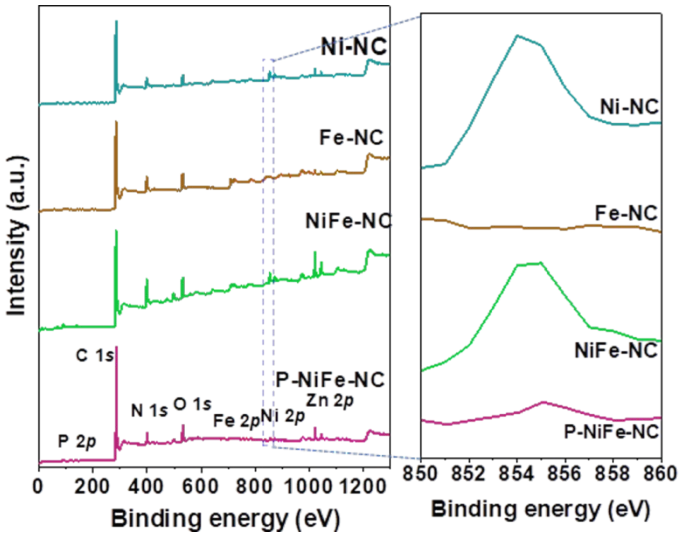

Fig. S5 XPS survey spectra of Ni-NC, Fe-NC, NiFe-NC and P-NiFe-NC.

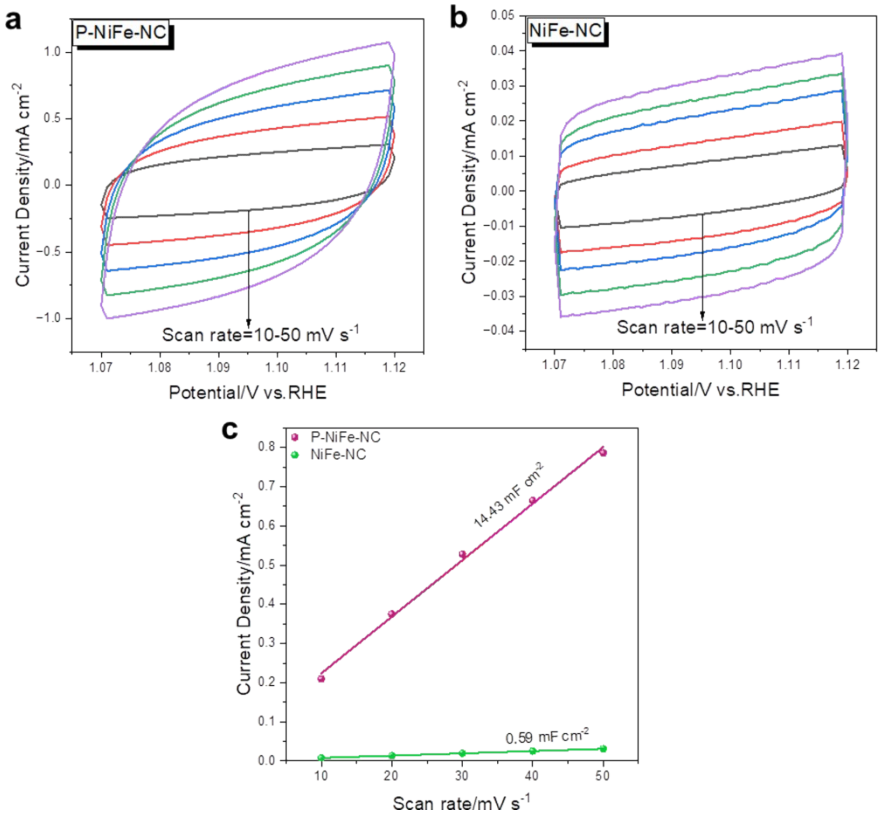

Fig. S6 CV curves of (a) P-NiFe-NC and (b) NiFe-NC with various scan rates. (c) Comparison of the electrochemical double-layer capacitance of P-NiFe-NC and NiFe-NC.

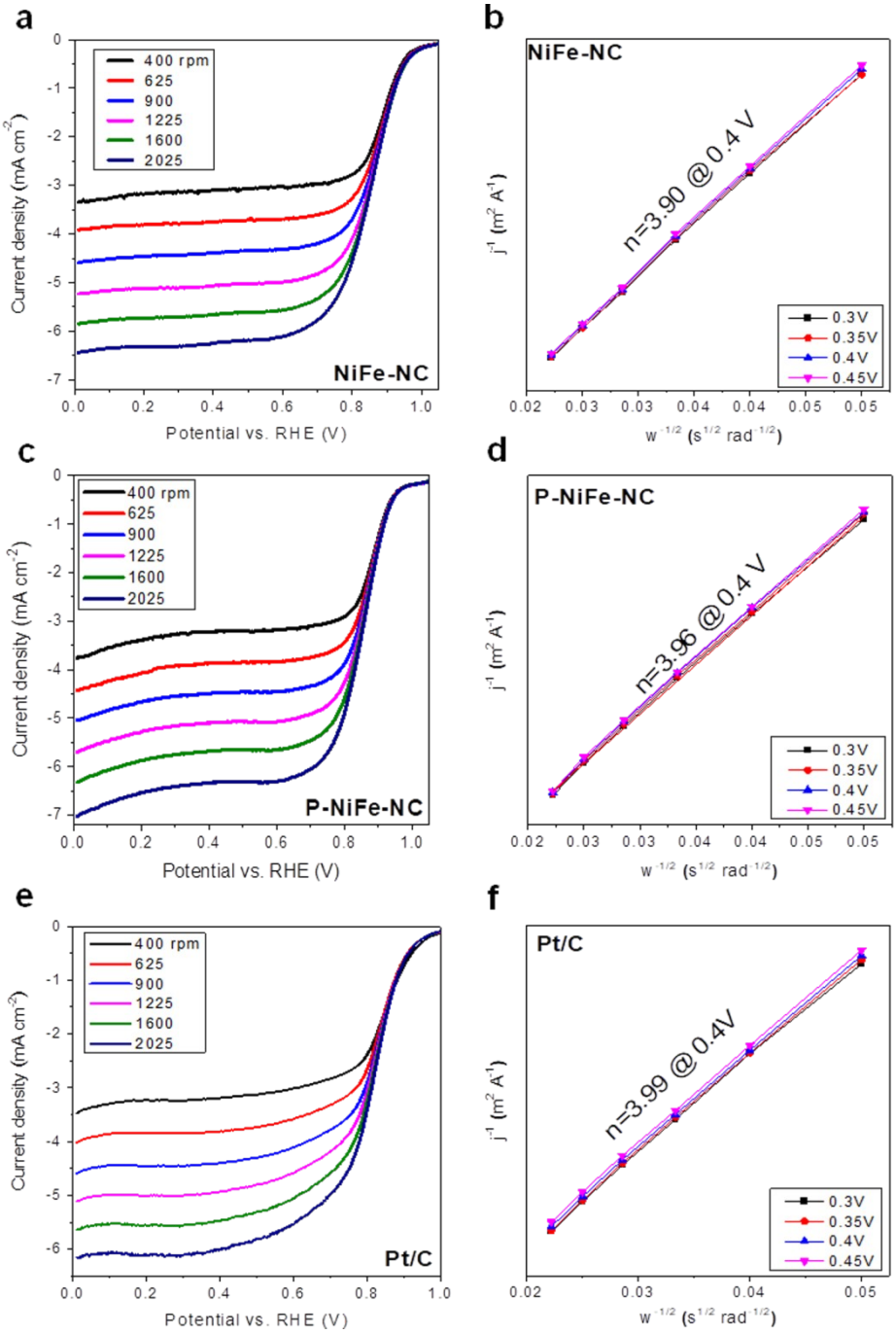

Fig. S7 ORR polarization curves of (a) NiFe-NC, (c) P-NiFe-NC, and (e) Pt/C at different rotation speeds. K-L plots of (b) NiFe-NC, (d) P-NiFe-NC, and (f) Pt/C at different potentials.

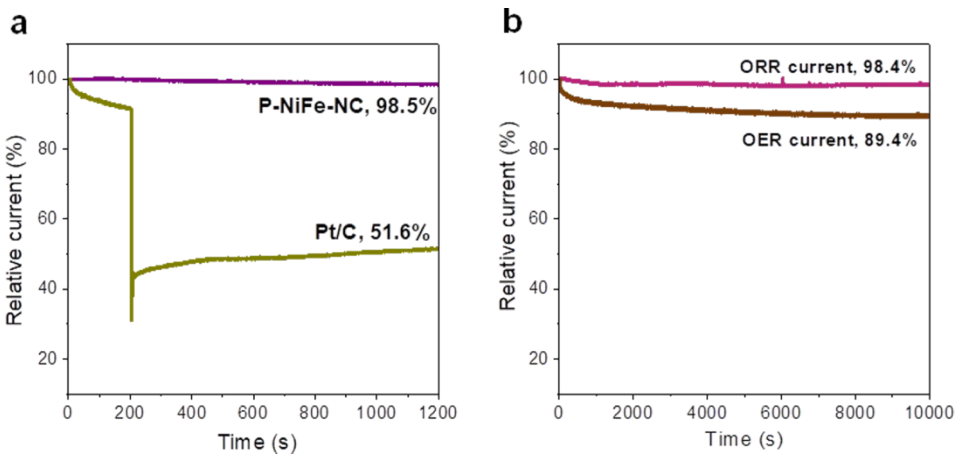

Fig. S8 (a) Methanol crossover tests of P-NiFe-NC and Pt/C. (b) Long-term durability curves of P-NiFe-NC for ORR and OER at potential of 0.6 and 1.69 V. respectively.

Table S1. Elemental contents of P-NiFe-NC and NiFe-NC

Element	P-NiFe-NC (at%)	NiFe-NC (at%)
C	88.47	76.94
N	6.69	14.76
O	3.27	6.89
Fe	0.49	0.48
Ni	0.90	0.93
P	0.18	-